U-Pb Ages and Hf Isotopes in Zircons from Parautochthonous Mesozoic Terranes in the Western Margin of Pangea: Implications for the Terrane Configurations in the Northern Andes

Camilo Bustamante,[1,2,*] *Carlos J. Archanjo,*[1] *Agustín Cardona,*[3] *Andres Bustamante,*[4] *and Victor A. Valencia*[5]

1. Instituto de Geociências, Universidade de São Paulo, Rua do Lago 562, CEP 05508-080, São Paulo, São Paulo, Brazil; 2. Departamento de Ciencias de la Tierra, Universidad EAFIT, Carrera 49 No. 7 Sur-50, Medellín, Colombia; 3. Departamento de Procesos y Energía, Facultad de Minas, Universidad Nacional, Carrera 80 No. 65-223, Medellín, Colombia; 4. Departamento de Geologia, Universidade Federal de Pernambuco, Avenida da Arquitetura s/n, CEP 50740-540, Recife, Pernambuco, Brazil; 5. Department of the Environment, Washington State University, Pullman, Washington 99164, USA

ABSTRACT

U-Pb laser ablation inductively coupled plasma mass spectrometry ages and Hf isotopes in zircons were used to constrain the nature of two geological units representative of the basement of the Central Cordillera of Colombia. Graphite-quartz-muscovite schists from the Cajamarca Complex show inherited detrital zircons supplied mostly from Late Jurassic (ca. 167 Ma), Ediacaran (ca. 638 Ma), and Tonian (Grenvillian; ca. 1000 Ma) sources. These marine volcanosedimentary deposits form an N-trending metamorphic belt in fault contact to the east with orthogneisses and amphibolites of the Tierradentro unit. Zircon U-Pb determinations of the Tierradentro rocks—previously interpreted as Grenvillian basement slices—yielded crystallization ages between 271 and 234 Ma. Initial Hf data reveal that the Tierradentro unit shares isotopic characteristics similar to other Permo-Triassic rocks of the Central Cordillera. In contrast, inherited detrital zircons from the Jurassic metasedimentary rocks suggest that their sources are distinct from the plutonic rocks that crop out in the Central Cordillera with Jurassic crystallization ages. Large xenoliths of the Tierradentro unit within the Ibagué batholith indicate that the granodioritic magma mostly intruded a Permo-Triassic basement possibly by exploiting the Otú-Pericos fault. The Jurassic metasedimentary belt is correlated further south with a similar sequence in the Ecuadorian Andes named Salado terrane.

Online enhancements: supplemental tables.

Introduction

Continental margins are modified by the accretion of oceanic and continental terranes during subduction. While the allochthonous origin of oceanic terranes can be recognized by their particular tectonostratigraphic record, identifying continental terranes as transferred from another continental margin (allochthonous) or formed at the same continental margin and transferred by along-strike translation (i.e., parautochthonous) may be more complicated (Howell 1995).

The Northern Andean Belt evolved by accretion of continental and oceanic crustal fragments to the margin of South America by strike-slip faults and subduction zones, with some of the major periods of accretion occurring in the Permo-Triassic, Jurassic, and Late Cretaceous (Ramos 2009). The Permo-Triassic events have been recently characterized as related to the agglutination and rifting associated

Manuscript received February 5, 2016; accepted April 29, 2017; electronically published August 3, 2017.

* Author for correspondence; e-mail: cbustam3@eafit.edu.co.

[The Journal of Geology, 2017, volume 125, p. 000–000] 0022-1376/2017/12505-00XX$15.00. DOI: 10.1086/693014

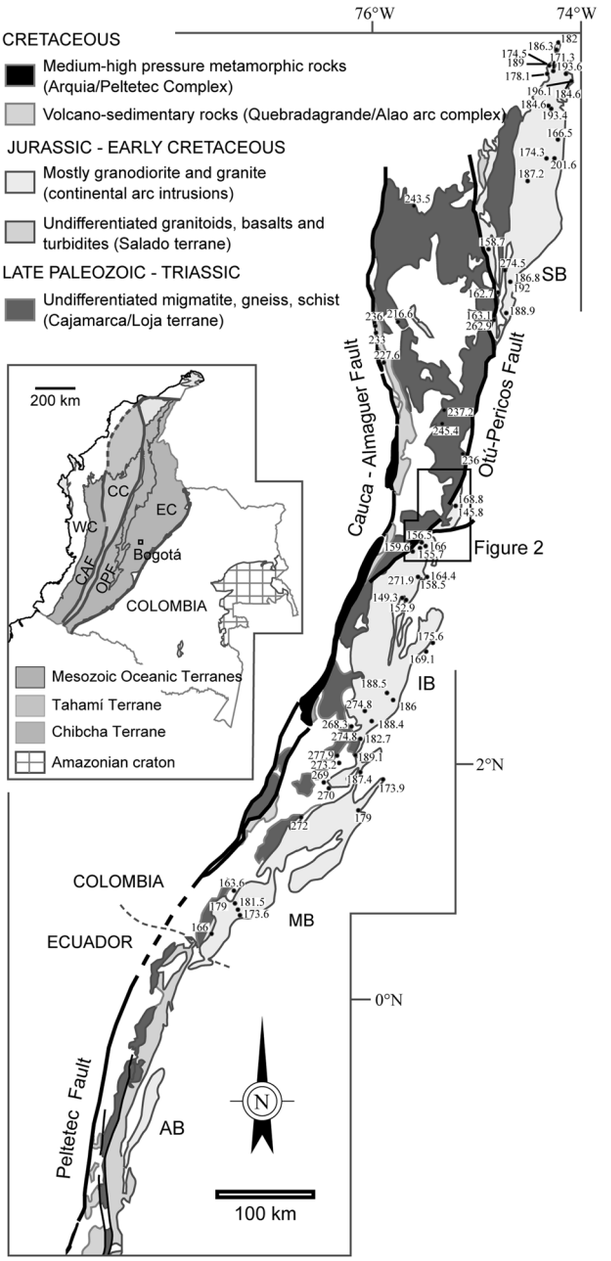

Figure 1. Geology of the Central Cordillera (CC) in Colombia and Cordillera Real in Ecuador, showing the distribution of Cretaceous metamorphic and volcanosedimentary rocks and Jurassic continental arc intrusions: Abitagua (AB), Ibagué (IB), Mocoa (MB), and Segóvia (SB) batholiths and Permo-Triassic rocks. Inset indicates main geological domains of Colombia highlighting the location of the Western (WC) and Eastern (EC) Cordilleras. Map shows the two tectonostratigraphic terranes studied: Chibcha to the east of the Otú-Pericos fault (OPF) and Tahamí to the west. Numbers represent Permo-Triassic and Jurassic age distribution along the Central Cordillera of Colombia. Ages were compiled from Vinasco et al. (2006), Restrepo et al. (2011), Blanco-Quintero et al. (2014), Cuadros et al. (2014), Martens et al. (2014), Spikings et al. (2015), Bustamante et al. (2016), Rodríguez et al. (2017), and Zapata-García et al. (2017). CAF = Cauca-Almaguer fault. A color version of this figure is available online.

with the formation and breakup of Western Pangea (Vinasco et al. 2006; Villagomez et al. 2011; Cochrane et al. 2014*a*). During the Jurassic, the margin was intruded by continental arc batholiths characterized in their earlier phases by a significant extensional signature (Sarmiento-Rojas et al. 2006; Cochrane et al. 2014*b*). Subsequently, the interactions of the Caribbean, Pacific, and South American plates in the Cretaceous lead to bulk compression of the continental margin, accretion of oceanic terranes, and lateral migration of crustal blocks along strike-slip faults (Bayona et al. 2006; Pindell and Kennan 2009; Spikings et al. 2015).

Restrepo and Toussaint (1988) and Restrepo et al. (2011) adopted the tectonostratigraphic terrane model of Coney et al. (1980) to divide the accretionary sequences of the Colombian Andes into four major terranes. They comprise an allochthonous Chibcha terrane adjacent to the Precambrian Guiana and Amazonian shields that outcrops in the Eastern Cordillera and the Magdalena river valley, separated by other allochthonous units exposed in the Central and Western Cordilleras (fig. 1). In the Central Cordillera, they recognized a Late Paleozoic to Triassic Tahamí terrane bounded to the east by the Otú-Pericos fault and to the west from Cretaceous oceanic-related terranes by the Romeral Fault System.

The origin of these terranes—and particularly the age of tectonomagmatic events of the Tahamí and Chibcha terranes as well as their limits—and their allochthonous or autochthonous nature has been intensely debated (Cardona-Molina et al. 2006; Vinasco et al. 2006; Restrepo et al. 2011; Blanco-Quintero et al. 2014; Martens et al. 2014; Spikings et al. 2015). According to Restrepo and Toussaint (1988) and Toussaint and Restrepo (1989), one of the major distinctions between Tahamí and Chibcha terranes are Late Paleozoic tectonometamorphic events just recorded in the former and the Jurassic magmatism and sedimentation that is found only in the Chibcha terrane (Restrepo et al. 2011). Jurassic metasedimentary rocks, however, have been identified in the Cordillera Real of Ecuador (Salado terrane) next to the Peltetec fault (Litherland et al. 1994; Spikings et al. 2015). Furthermore, Permo-Triassic gneisses and migmatites have been recently identified to the east of the Otú-Pericos fault (Villagómez et al. 2011; Cochrane et al. 2014*a*; Rodríguez et al. 2017), and Jurassic metamorphism of rocks formerly attributed to the Permian to Triassic Cajamarca Complex has

been identified to the west of the Ibagué batholith (Blanco-Quintero et al. 2014). These recent results therefore challenge the identification of the Otú-Pericos fault as the terrane boundary separating Grenvillian and Permo-Triassic basement in Colombia. Consequently, the definition of Tahamí and Chibcha as allochthonous terranes on the basis of the criteria outlined by Restrepo and Toussaint (1988) needs to be reconsidered.

Our study examines the geological evolution of units on both sides of the Otú-Pericos fault near the northern termination of the Ibagué batholith (fig. 1). We present new zircon U-Pb laser ablation inductively coupled plasma mass spectrometry (LA-ICP-MS) and Hf isotope data for orthogneisses and amphibolites from a geological unit known as the Tierradentro sequence and detrital zircons from pelitic schist within the Tahamí terrane. The Tierradentro sequence has been mapped as slices of Grenvillian rocks (ca. 1 Ga) that bound the Chibcha Terrane (fig. 2). Our data show that the Tierradentro gneisses and amphibolites are not Grenvillian rocks, while the metapelites included in the Cajamarca Complex record a peak detrital zircon population at ca. 166 Ma. These results suggest that the Otú-Pericos fault may represent a more complicated structure, which seems to limit distinct tectonostratigraphic sequences of the same age with contrasting histories. The new results also confirm the existence of metasediments with Jurassic protoliths in the Central Cordillera, which has just recently been documented (Blanco-Quintero et al. 2014), and suggest a more complicated Jurassic tectonic record.

Geological Setting

The Andes in Colombia are composed of three mountain ranges: the Western, Central, and Eastern Cordilleras (fig. 1, inset). The Western Cordillera comprises allochthonous oceanic rocks that accreted to the continental margin since the Late Cretaceous (Kerr et al. 1997; Villagómez et al. 2011). The Eastern Cordillera comprises a basement composed of Precambrian gneisses, granulites, and amphibolites and Ordovician to Silurian granitoids that are covered by Paleozoic transitional siliciclastic and carbonate deposits (Kroonenberg 1982; Restrepo-Pace et al. 1997; Cordani et al. 2005; Cardona-Molina et al. 2006; Ordóñez-Carmona et al. 2006; van der Lelij et al. 2016). A major Late Carboniferous tectonic event has been discriminated on the basis of a major Pennsylvanian hiatus and the existence of some angular discordance with the Permian (Toussaint 1995). The latter form the Chibcha terrane, which is limited to the east by the Guaicáramo fault. Isolated Proterozoic inliers to the southeast of the Guaicáramo fault are considered as a prolongation of the South American continental margin (Putumayo orogen; Ibañez-Mejia et al. 2011). In turn, the Central Cordillera consists of Permian to Triassic I-type magmatic rocks, migmatites, and amphibolites (Vinasco et al. 2006; Cochrane et al. 2014*a*; Spikings et al. 2015) grouped in the Cajamarca Complex (Maya and González 1995). The Permo-Triassic units of the Central Cordillera have been correlated in Central America with the Mexican terranes, which were formed in a continental arc (Torres et al. 1999; Dickinson and Lawton 2001). Further south in Ecuador, they were correlated with Triassic S-type granitoids and metamorphic rocks of the Loja Terrane in the Cordillera Real (Noble et al. 1997; Riel et al. 2013; Spikings et al. 2015).

The high- to medium-grade rocks of the Cajamarca Complex are intruded by Triassic S-type granitoids that form the basement sequence of the Central Cordillera, with the age of its metamorphism varying from Mid- to Late Triassic (ca. 240–230 Ma; Vinasco et al. 2006; Restrepo et al. 2011; Cochrane et al. 2014*a*).

In the Ibagué area to the south of the Central Cordillera (fig. 2), Jurassic to Cretaceous plutons (i.e., Ibagué batholith and Mariquita stock) and Eocene magmatic rocks intrude the metasedimentary rocks included in the Cajamarca Complex. According to Blanco-Quintero et al. (2014), the peak metamorphic conditions determined in garnet-biotite schists reached 550°–580°C and 8 kbar, while $^{40}Ar/^{39}Ar$ determinations in amphibole and phengite between 146 and 158 Ma defined the age of the peak metamorphic conditions. These Late Jurassic ages contrast with previous Triassic metamorphism of the Cajamarca Complex, which led Blanco-Quintero et al. (2014) to propose a distinct Late Jurassic collision-accretion event in the Central Cordillera. Similarly, in southernmost Colombia, Zapata-García et al. (2017) have suggested the existence of a metamorphic event between 163 and 169 Ma that affected metasedimentary rocks on the basis of U-Pb zircon geochronology.

The Tierradentro gneisses and amphibolites are located to the east of the Otú-Pericos fault (Restrepo et al. 2011; fig. 2). These poorly studied rocks have been correlated with the Proterozoic basement of the eastern flank of the Central Cordillera (Kroonenberg 1982; Restrepo-Pace et al. 1997) on the basis of lithological similarities (Marquinez and Núñez 1998; Núñez 2001) and a K-Ar age of 1360 ± 270 Ma (Vesga and Barrero 1978) and therefore have been included as part of the Chibcha Terrane. The Tierradentro unit is composed of discontinuous lenses of ortho- and paragneisses, amphibolites, minor granulites, and

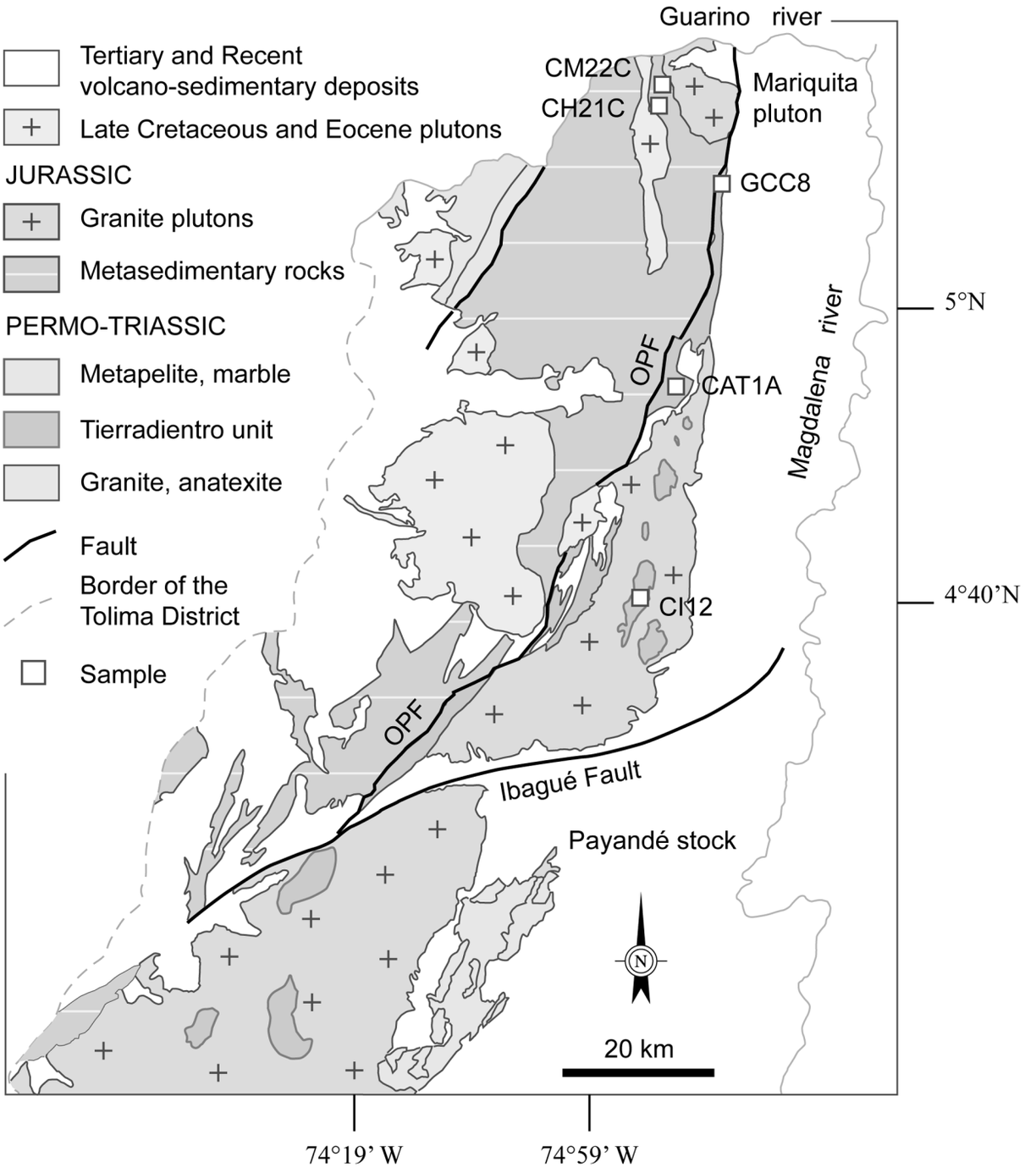

Figure 2. Detailed geological map of the study area, showing sample distribution (squares) and relations between the studied units. The Otú-Pericos fault (OPF) divides the Chibcha terrane (east) from the Tahamí (west). Note that we are considering Permo-Triassic and Jurassic components on both sides of the fault, contrary to the original definitions of those terranes. A color version of this figure is available online.

marbles that form both the host rocks and enclaves of the northern part of the Ibagué batholith (fig. 2). The batholith shows zircon U-Pb ages ranging from 142 to 170 Ma (Leal-Mejía 2011; Villagómez et al. 2011; Bustamante et al. 2016). The wall rocks to the east of the batholith include Triassic limestones intruded by the Payandé stock (ca. 165 Ma; Bustamante et al. 2016). Anatexites close to the Payandé stock provided zircon U-Pb ages of ca. 230 Ma, which is the first Triassic ages reported to the east of the Otú-Pericos fault (Cochrane et al. 2014*a*).

Analytical Methods

LA-ICP-MS U-Pb Geochronology in Zircon. Heavy mineral concentrates of the <350-μm fraction were separated using traditional techniques. Zircons from the nonmagnetic fraction were handpicked under the microscope and mounted in a 1-inch-diameter epoxy puck and slightly ground and polished to expose the surface and keep as much material as possible for laser ablation analyses. After cathodoluminescence (CL) imaging, the LA-ICP-MS U-Pb analyses were conducted using a New Wave Nd:YAG ultraviolet 213-nm laser coupled to a ThermoFinnigan Element 2 single-collector, double-focusing magnetic sector ICP-MS at Washington State University. Operating procedures and parameters are described in detail by Chang et al. (2006) and Gaschnig et al. (2010) and are only summarized here. Laser spot size and repetition rate were 30 μm and 10 Hz, respectively. He and Ar carrier gases delivered the sample aerosol to the plasma. Each analysis consists of a short blank analysis followed by 250 sweeps through masses 202, 204, 206, 207, 208, 232, 235, and 238, taking approximately 30 s. Fractionation was corrected by normalizing U/Pb and Pb/Pb ratios of the unknowns to the zircon standards (Chang et al. 2006). U and Th concentration were monitored by comparing with National Institute of Standards and Technology 610 trace element glass. Zircon standard Plešovice was used, with an age of 337.13 ± 0.37 Ma (Sláma et al. 2008). Uranium-lead ages were calculated using Isoplot 4.15 (Ludwig 2003) and are presented in table S1 (tables S1, S2 are available online).

Hf Isotopes in Zircon. Hf isotope geochemistry analysis was performed on three samples (table S2) at the Geoanalytical Lab at Washington State University, using a ThermoFinnigan Neptune multicollector ICP-MS equipped with nine faraday collectors interfaced with a New Wave 213-nm UP Nd:YAG laser. Laser spot size was 40 μm, and the data were acquired in static mode with 60-s integrations. Details of analytical procedures and data treatment

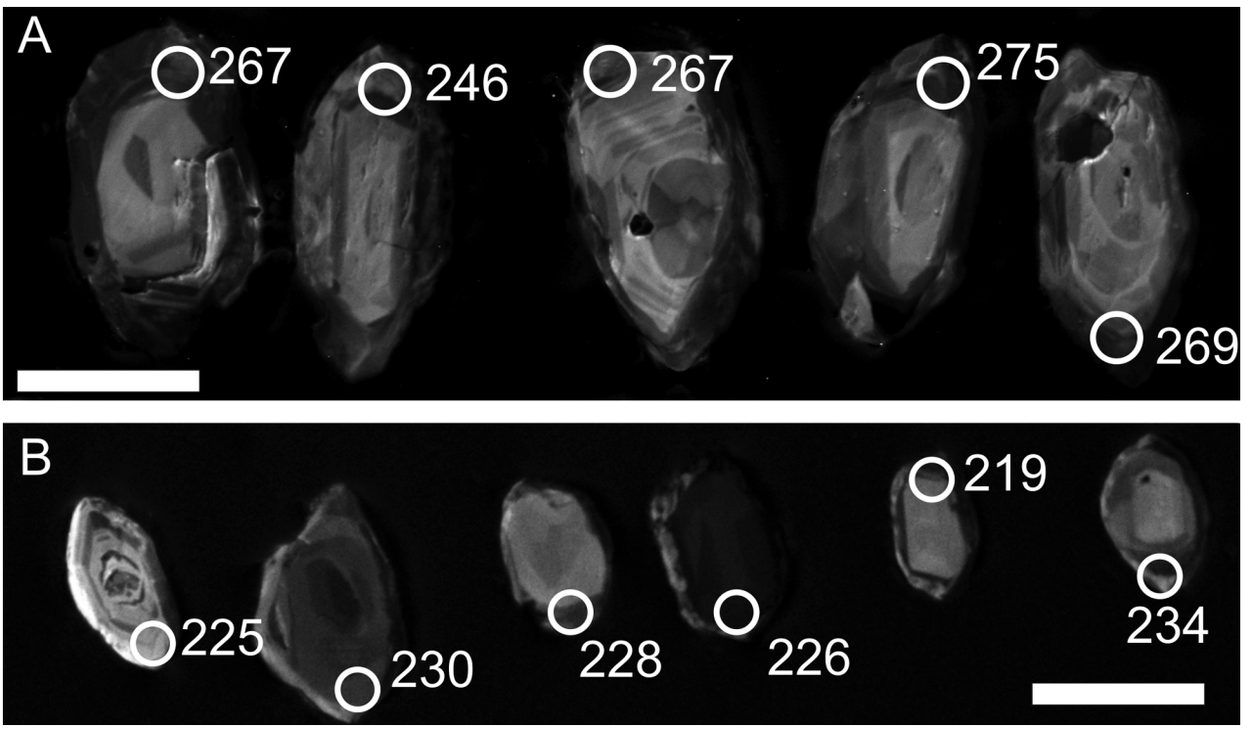

Figure 3. Cathodoluminescence (CL) images from selected zircons of the studied samples showing the analyzed spots and U-Pb ages obtained. *A*, Sample CI12 (orthogneiss). *B*, Sample CAT1A (amphibolite). Scale bars = 100 μm.

follow those of Vervoort et al. (2004) and DuFrane et al. (2007). For the Hf depleted mantle model ages (Hf_{TDM}), we used $^{176}Hf/^{177}Hf$ and $^{176}Lu/^{177}Hf$ for the individual zircon samples to determine their initial $^{176}Hf/^{177}Hf$ ratios at their crystallization ages. Projection back from zircon crystallization was calculated using a present value of 0.0150 for the estimated $^{176}Lu/^{177}Hf$ of continental crust (Vervoort and Patchett 1996; Goodge and Vervoort 2006). The depleted mantle Hf evolution curve was calculated from present-day depleted mantle values of $^{176}Hf/^{177}Hf$ $DM_{(0)} = 0.283240$ and $^{176}Lu/^{177}Hf$ $DM_{(0)} = 0.03979$ (Vervoort et al. 2015).

Results

Tierradentro Unit. The samples (see location in fig. 1) of the Tierradentro unit comprise an orthogneiss (GCC8) and an amphibolite (CAT1A) exposed in faulted contact with micaschists and an orthogneiss (CI12) that crops out as a roof pendant within the Ibagué batholith. The orthogneiss (CI12) that forms a roof pendant within the Ibagué batholith is composed of plagioclase An_{12} (34%), orthoclase (28%), quartz (22%), hornblende (11%), and biotite (5%). The secondary phases are included as products of saussuritization and sericitization processes at the core and rims, respectively, in plagioclase grains. Prenhite occurs in veins cutting the sample and chlorite as a pseudomorphic phase after biotite. Accessory phases include zircon, apatite, titanite, and opaque minerals. The gneiss shows a foliation defined by recrystallized quartz ribbons surrounded by hornblende and plagioclase. Quartz has sutured boundaries and undulatory extinction. The amphibole also appears as porphyroblasts with minor portions replaced by chlorite and calcite, mainly along the cleavage planes. Mineral assemblages suggest that the sample reached the amphibolite facies and the protolith corresponds to an intermediate igneous rock.

Zircons of the quartz-feldspathic gneiss range from 70 to 300 μm in length. They are mainly subhedral, mostly with subrounded to rounded terminations. CL images record a faint oscillatory zoning close to the border as well as in the center of some zircons (fig. 3*A*). Th/U ratios of the grains vary from 0.47 to 1.04 (table S1), suggesting that they are magmatic zircons (Rubatto 2002).

U-Pb analyses were performed on 48 zircons. After removing from the calculations zircons with >10% discordance, the analysis provided a $^{206}Pb/^{238}U$ mean age of 271.3 ± 1.3 Ma (fig. 4). There is no significant age difference between the U-Pb ages in cores and their respective rims in the zircons of the

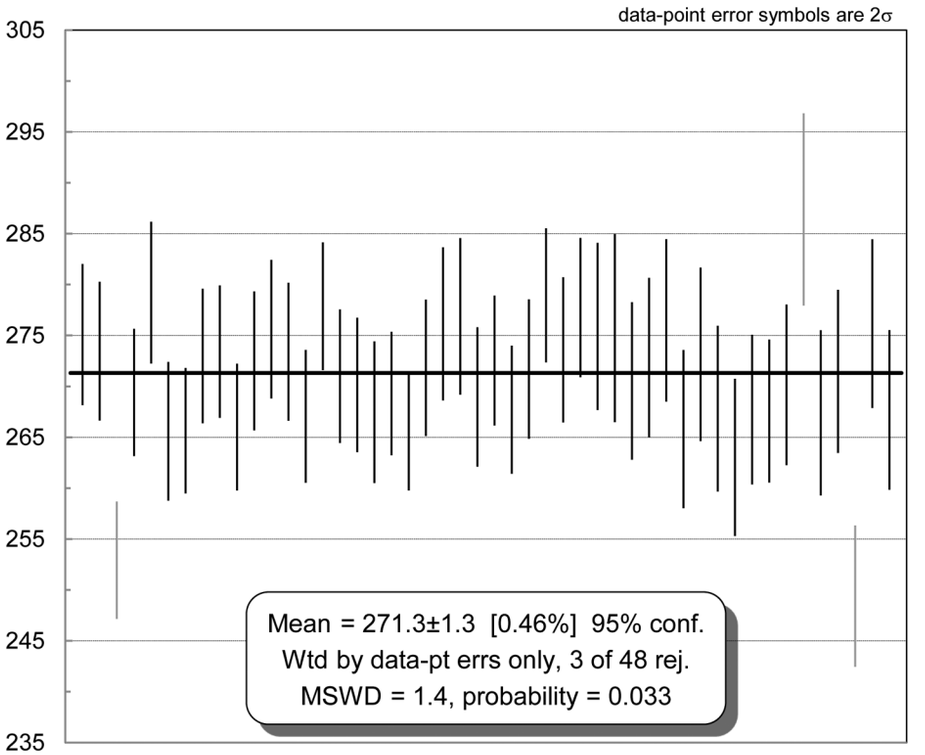

Figure 4. $^{206}Pb/^{238}U$ mean age from zircon rims representing igneous crystallization age of sample CI12 (orthogneiss).

quartz-feldspathic gneiss. These results indicate that the zircons record the age of the igneous crystallization of the protolith and that they were not affected by late metamorphic events, as suggested by the absence of overgrowths observed in CL images.

The amphibolite (CAT1A) is made up of hornblende (61%), plagioclase An_{36} (27%), and quartz (12%). Secondary minerals include mainly muscovite as a product of retrograde metamorphism of plagioclase and chlorite replacing hornblende. Normal zoning of plagioclase is detected by the saussuritization at the core and sericitization in the rims. The sample exhibits a nematoblastic texture defined by the hornblende crystals orientation, and several mylonitic textures are observed, such as recrystallized and mortar quartz and deformed plagioclase twin systems. On the basis of the mineralogical analyses, this sample experienced amphibolite facies with an igneous rock with intermediate composition as the protolith.

Zircons from this amphibolite sample are anhedral to subhedral, mostly with rounded terminations but a few prismatic grains. Their sizes range from 60 to 250 μm in length (fig. 3*B*). CL images show zircons usually with dark, U-rich cores rimmed by lighter rims (fig. 3*B*). A few grains, however, display light U-poor cores surrounded by darker rims. However, no significant differences were found in Th/U ratios and ages after analyzing cores and rims of the zircons.

Thirteen zircons of the amphibolite (CAT1A) provided a $^{206}Pb/^{238}U$ mean age of 234.1 $\pm$ 5.3 Ma (fig. 5). The age calculation was obtained after discarding >10% discordant zircons. One individual zircon with a younger age (ca. 200 Ma) was attributed to Pb loss. Th/U ratios are relatively low, ranging from 0.12 to 0.25, with a few grains with even lower values. The mean age is interpreted as the magmatic crystallization of the zircon, which shows Th/U ratios that are systematically higher than 0.1 (Rubatto 2002). Similar ratios were found by Cochrane et al. (2014*a*) in Permo-Triassic amphibolites from the Central Cordillera of Colombia, where fractionation of U with respect to Th was described as the main cause for lowering Th/U ratios.

A mylonitized augen granodiorite (GCC8) was described in the hand sample. It is composed of plagioclase (50%), quartz (20%), K-feldspar (15%), biotite (10%), and muscovite (5%). The latter was associated with the main deformational fabric, whereas the K-feldspar is found as augen porphyroclasts.

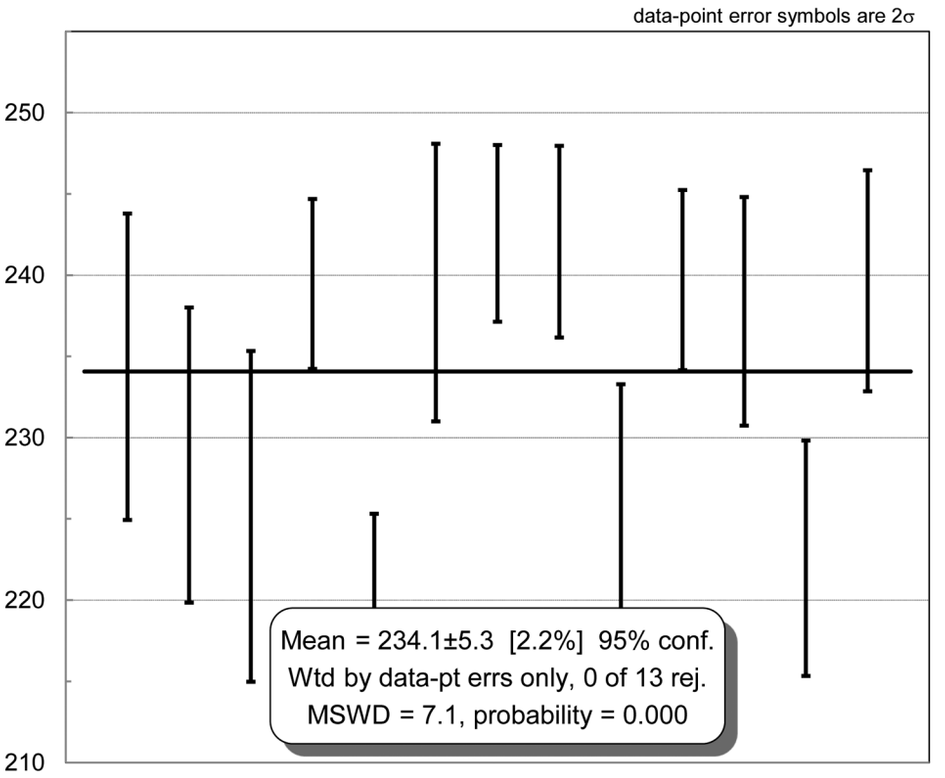

Figure 5. $^{206}Pb/^{238}U$ mean age from zircon rims representing igneous crystallization age of sample CAT1A (amphibolite).

Thirteen zircons of the orthogneiss (GCC8) yielded a $^{206}Pb/^{238}U$ crystallization age of 244.3 ± 4.8 Ma (fig. 6). Ages were obtained after removing >10% of discordant zircons.

Inherited Detrital Zircons of the Tahamí Terrane. Two schist samples were obtained from the Tahamí Terrane (see locations on fig. 2). The schist is intruded by Late Jurassic to Early Cretaceous Mariquita Stock (U-Pb crystallization age of ~130 Ma) that intrudes sampling locality CM22C and the Eocene Hatillo Stock (U-Pb crystallization age of ~54 Ma) that intrudes the locality in which sample CH21C was collected. However, zircons were obtained from only sample CH21C. Sample CM22C is described for reference.

Sample CH21C is graphite-quartz-muscovite schists. It is composed of muscovite (44%), quartz (34%), graphite (15%), biotite (3%), plagioclase (2%), and andalusite (2%). Accessories include apatite, zircon, and opaque minerals. Tourmaline is found as a trace mineral. Schistosity is defined by oriented micas with recrystallized quartz, which form a granolepidoblastic texture. Andalusite is also oriented along with micas. Decussate texture defined by postkinematic biotite indicates a possible superimposed contact metamorphic event. Epidote and muscovite appears locally as an alteration product. With the mineral association of this sample, it is possible to propose a greenschist facies of metamorphism and pelite sediment as the protolith for the analyzed sample.

Eighty-four zircons were extracted from the micaschist (table S1). The grains exhibit oscillatory zoning and have mainly subrounded to rounded terminations. Sizes range from 40 to 100 μm, although a few crystals can reach ~170 μm in length. The analyses comes from the zircon margin; some analyses, however, were obtained in the cores to check the possible multistage evolution of the zircons. Probability density plots are presented from a 100–800 Ma age interval, and >30% discordant zircons were not considered in the analysis.

Th/U ratios of the grain population range from 0.13 to 2.07, which are typical of magmatic zircons (Rubatto 2002). Three zircons with Proterozoic ages have Th/U ratios of ~0.04, which suggests a metamorphic origin. The major zircon population, however, shows Middle Jurassic (~167 Ma) and Ediacaran (~638 Ma) ages, with the youngest detrital zircon set at 162.5 ± 1.8 Ma (fig. 7). A few zircons display Paleozoic (Or-

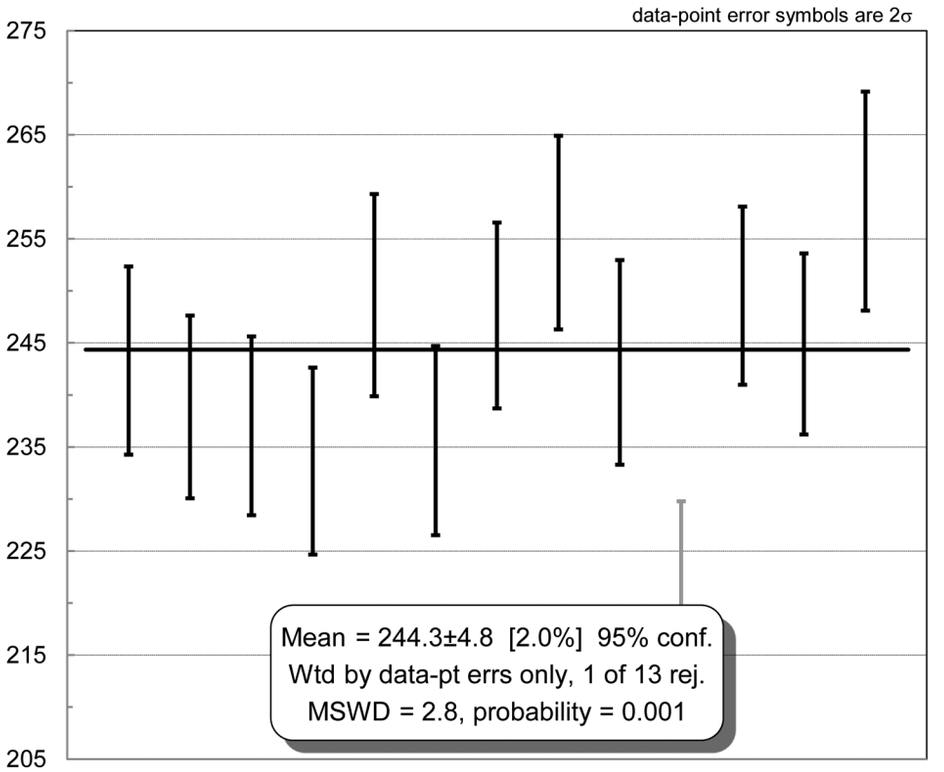

Figure 6. $^{206}Pb/^{238}U$ mean age from zircon rims representing igneous crystallization age of sample GCC8 (augen granodiorite).

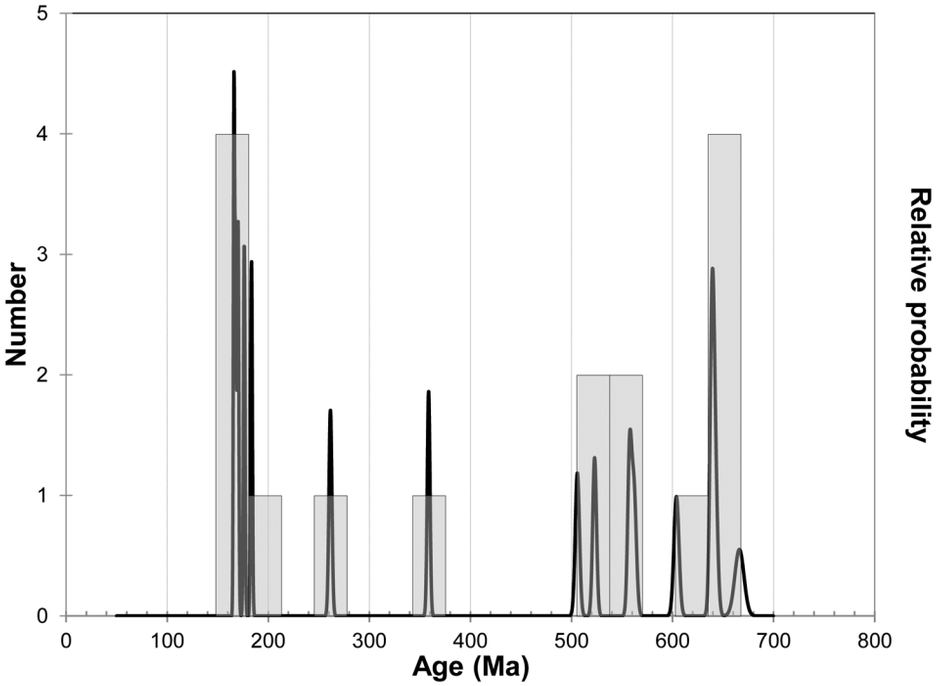

Figure 7. Probability density plot from inherited detrital zircons from the quartz-muscovite schist (CH21C). Plot shows grains with less than 30% of discordance and an age interval of 100–800 Ma. Note the important Middle Jurassic population. Maximum depositional age is 162.5 ± 1.8 Ma, given by the youngest zircon.

dovician and Carboniferous), Mesoproterozoic (Grenvillian), and Paleoproterozoic (Siderian and Statherian) ages. Permo-Triassic zircons are represented by one grain showing Triassic (~245 Ma) and one grain with Permian (~281 Ma) concordant ages.

Sample CM22C is a plagioclase-hornblende schist composed of hornblende (63%), plagioclase An_{32} (25%), and quartz (10%). Clinozoisite veins crosscut the foliation, which is defined by alternating bands of recrystallized plagioclase-quartz and oriented hornblende. Several clinozoisite grains are also accompanying the foliation of the rock. Opaque minerals (2%) as ilmenite and magnetite are observed as disseminated phases in the sample. Fine-grained muscovite is also observed as a replacement product of plagioclase. These alternating bands, in turn, define a granonematoblastic texture in the rock. The mineralogical composition suggests that the sample reached amphibolite facies and the protolith was an igneous rock with intermediate composition.

Hf Isotope Geochemistry. *Tierradentro Unit.* Hf isotopes were measured in the rims of eight zircons from samples CI12 (quartz-feldspathic gneiss) and CAT1A (amphibolite). Contrasting values were obtained on these samples. Initial ε_{Hf} values range from −0.1 to −2.5 for the orthogneiss, which suggests a crustal source for the protolith (fig. 8*A*). The amphibolite yielded initial ε_{Hf} values ranging from +9.2 to +10.9, indicating a mantle source for the protolith with values close to the depleted mantle curve (fig. 8*A*). Cochrane et al. (2014*a*) in other Permo-Triassic localities of the Central Cordillera obtained similar values.

Inherited Detrital Zircons of the Tahamí Terrane. We analyzed 28 zircons covering the U-Pb age range of the micaschist but with an emphasis on the Jurassic zircons. Hf isotopes from the older zircons usually show strong involvement of an old crustal component (fig. 8*B*). $\varepsilon_{Hf(i)}$ for the oldest zircons is −8.2 and −0.7 (Siderian and Statherian, respectively). For the Grenvillian zircons, $\varepsilon_{Hf(i)}$ is −0.3 and −4.3, with crystals showing a juvenile value of +2.5. Two Ediacaran zircons have $\varepsilon_{Hf(i)}$ of −7.4 and −8.0, and two yielded slightly juvenile values of +0.7 and +1.8. Paleozoic (Ordovician and Carboniferous) zircons show values from −19.9 to −1.2. $\varepsilon_{Hf(i)}$ values of nine Jurassic zircons (fig. 8*A*) provided three zircons with positive values ranging from +0.5 to +2.8, and six zircon yielded values between −0.3 and −3.0 (table S1; fig. 8).

Discussion

U-Pb zircon ages indicate that the protoliths of the Tierradentro orthogneiss and amphibolite crystallized

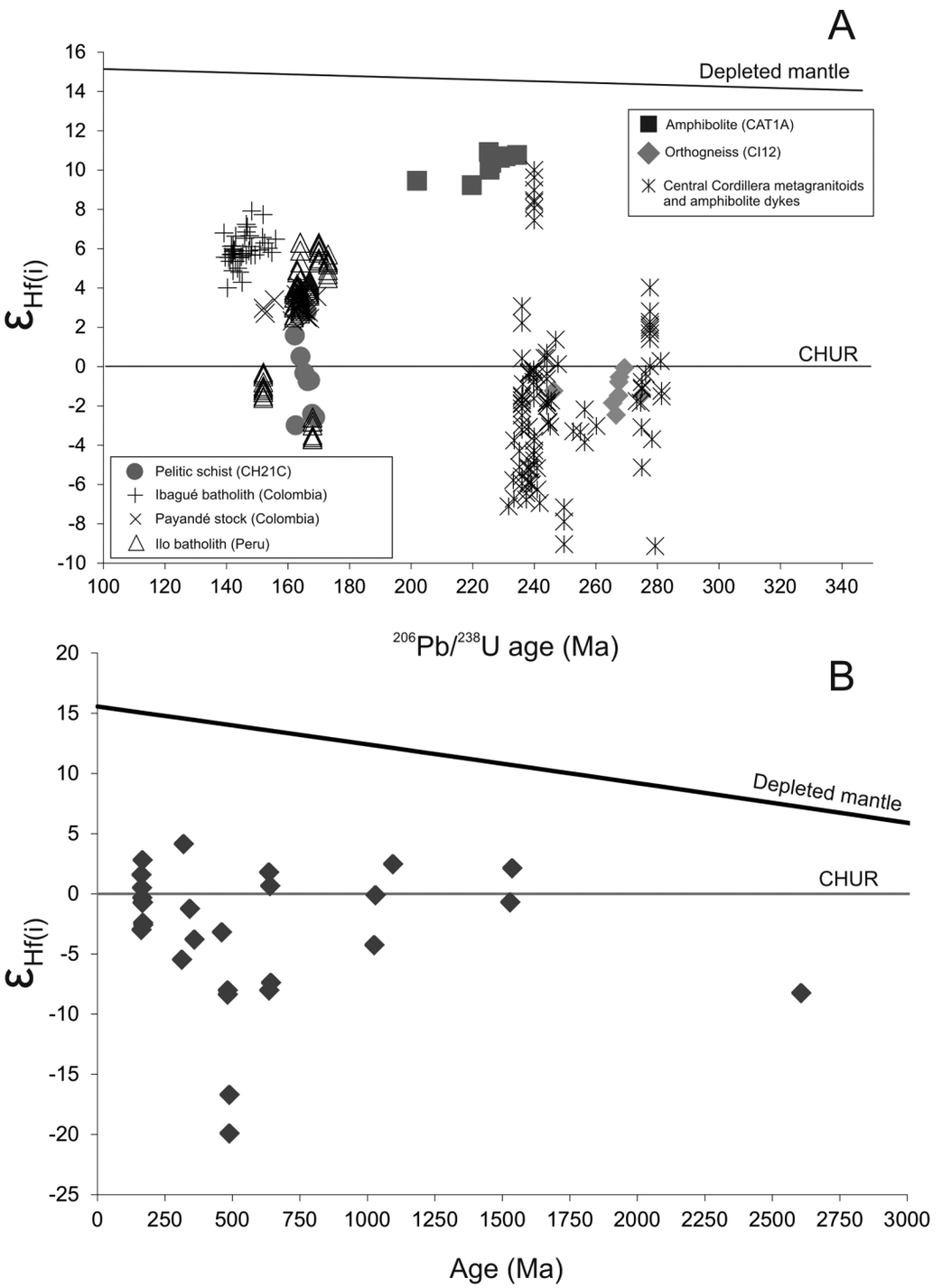

Figure 8. *A*, Initial ε_{Hf} versus $^{206}Pb/^{238}U$ age diagram. Squares represent zircons from sample CAT1A (amphibolite) with a strong juvenile signature, as opposed to zircons from sample CI12 (quartz-feldspathic gneiss; triangles), which reflects the involvement of crustal sources for this rock. Circles are from detrital zircons of the Tahamí terrane. See comparison with published data from other Middle Jurassic plutons of the Central and Northern Andes (Ilo batholith: Boekhout et al. 2012; Payandé and Ibagué plutons: Cochrane et al. 2014*b*; Bustamante et al. 2016). *B*, Distribution of the $\varepsilon_{Hf(i)}$ obtained for the Cajamarca Complex in this study. A color version of this figure is available online.

in the Permo-Triassic (ca. 271–234 Ma). The orthogneiss exposed as a roof pendant within the Ibagué batholith yielded initial ε_{Hf} from −0.1 to −2.5 and show a component that is more characteristic of a mix with older radiogenic continental crust input. The amphibolite, in contrast, provided initial ε_{Hf} from +9.2 to +10.9 to indicate a juvenile mantle derived source. These data are similar to those obtained in different regions of the basement rocks of the Central Cordillera and Ecuador that are attributed to a geodynamic setting that includes Permo-Triassic rifting with associated bimodal magmatism related to continental breakup succeeded by subduction of the proto-Pacific (Cardona et al. 2010; Villagómez et al. 2011; Cochrane et al. 2014*a*). Our results therefore show that not all the Tierradentro rocks are Grenvillian in age, as previously considered, and that accordingly the walls of the Jurassic Ibagué batholith were formed in the Permo-Triassic. The volume of Precambrian rocks in the Chibcha terrane (eastern flank of the Central Cordillera) therefore also appears to be overstated (Kroonenberg 1982; Restrepo-Pace et al. 1997). The only reliable Precambrian rocks of the Central Cordillera are the Mesoproterozoic sequences documented in the San Lucas Range, located close to the northern border of the Jurassic Segovia batholith (Cuadros et al. 2014).

Permo-Triassic gneisses, migmatites, amphibolites, and metasedimentary rocks have been considered as a major element of the Cajamarca Complex and the Tahamí Terrane (Restrepo and Toussaint 1988; Vinasco et al. 2006; Restrepo et al. 2011; Martens et al. 2014). Zircon crystallization ages of S-type granitoids and $^{40}Ar/^{39}Ar$ amphibole cooling ages indicate that the high-grade metamorphism of the northern part of the Cajamarca Complex occurred in the Mid- to Late Triassic (Vinasco et al. 2006; Cochrane et al. 2014*a*).

In the central portion of the Central Cordillera (~5°N), the Otú-Pericos fault marks the contact of the Tierradentro gneisses and amphibolites (east) with pelitic schists deposited in the Jurassic (west). Further south the Tierradentro unit pinches out and the Otú-Pericos fault defines the western contact of the Ibagué batholith. We envisage that the Ibagué batholith intruded mostly Permo-Triassic orthogneisses and amphibolites. The granitic magma would have moved upward to incorporate, during the ascent, xenoliths of variable sizes of the Tierradentro unit. Smaller Jurassic–Early Cretaceous plutons, such as the Payandé stock and the Mariquita pluton, intruded, respectively, the Late Triassic calcareous rocks located east of the Otú-Pericos fault and amphibole schists (sample CH21C; fig. 2). Permo-Triassic rocks found on both sides of the Otú-Pericos fault agree with recent data reported in the Central Cordillera that put into question the reliability of the terrane discrimination analysis that used contrasting Mesozoic basement history as the major criteria for the terrane model (Villagómez et al. 2011; Blanco-Quintero et al. 2014; Cochrane et al. 2014*a*; Spikings et al. 2015; Rodríguez et al. 2017; Zapata-García et al. 2017). However, Blanco-Quintero et al. (2014) have identified a Jurassic (158–147 Ma) metamorphism based on $^{40}Ar/^{39}Ar$ plateau ages in mica and amphiboles from schists and amphibolites, which contrasts with the Triassic metamorphism of the Cajamarca Complex defined in the northern part of the Central Cordillera.

Our results confirm the presence of Mesozoic ages in the metamorphic rocks of the Central Cordillera formerly considered as the Cajamarca Complex. The new data suggest the existence of a Jurassic depositional basin floored by Permo-Triassic rocks that was fed by detrital zircons supplied in part by the erosion of Jurassic sources, highlighting the importance of the Jurassic events in the assembly of the Central Cordillera, with important correlations with the Ecuadorian Cordillera Real (Vanegas et al. 2014). The Jurassic metavolcanosedimentary belt in the Tolima State, including the area defined by Blanco-Quintero et al. (2014), forms an N-trending elongated sequence in fault contact with Permo-Triassic rocks (fig. 2) as well as the southern expression of the Jurassic metamorphism (Zapata-García et al. 2017). This fault system corresponds to the Otú-Pericos and the Chusma-Algeciras that was used to define the eastern limit of the Tahamí terrane.

A critical aspect of the detrital zircon results relates to the source area of the Jurassic detrital zircons found in the metasedimentary rocks of the Cajamarca Complex. Although Middle to Late Jurassic magmatic rocks are common along the Ecuadorian and Colombian Andean margins (Cochrane et al. 2014*b*; Spikings et al. 2015; Bustamante et al. 2016), initial Hf isotopic signatures in detrital zircons from the mica schist are more radiogenic and differ from those recognized in the Jurassic magmatic belts that characterized the Northern Andes east of the Cajamarca Complex (fig. 8*A*). Their higher radiogenic values show some resemblance with magmatic rocks farther south, such as the Ilo batholith in Peru (south of ~5°S), which is emplaced in Precambrian crust (Boekhout et al. 2012). The presence of both Triassic and Jurassic magmatic record allows us to question the simple separation of the Tahamí and Chibcha terranes with age criteria. However, the radiogenic Hf isotopic signature found in the schist sample from the Cajamarca Complex suggests that the Jurassic source areas for the studied schist differed from the

eastern Jurassic magmatic rocks associated with the Chibcha Terrane (fig. 8*A*).

When the Jurassic tectonostratigraphic record is compared, a major difference also arises between the Chibcha and Tahamí terranes. Whereas the former records the growth of an arc setting (Bustamante et al. 2016), the latter experienced a metamorphic event apparently associated with a collisional setting (Blanco-Quintero et al. 2014) in a geothermal gradient that does not match with the high heat flux that characterized arc and backarc settings. Such contrasting tectonic scenarios separated by the Otú-Pericos fault suggest that their tectonic history cannot be explained by lateral variation of tectonic style (Howell 1995) and suggest a contrasting tectonic evolution. On the basis of these tectonostratigraphic constraints, we therefore suggest a series of different tectonic scenarios for the Triassic to Jurassic tectonic evolution of both terranes.

Triassic rocks from the Chibcha and Tahamí terranes are similar in character and age and therefore suggest that they experienced a common tectonic extensional evolution associated with the early Pangea breakup and the subduction of the Pacific plate (Cochrane et al. 2014*a*; this article). Several continental blocks may have been detached from some segments of the margin during this extensional event. During the Jurassic, several arcs were formed along different segments of the Northern Andean margin and the detached fragments. As suggested by Blanco-Quintero et al. (2014), during the Jurassic some segments of the Northern Andes experienced a collisional event, whereas others were experiencing continuous subduction with the growth of magmatic arcs.

The southern part of the Tahamí terrane in the Colombian Andes and the Salado terrane of the Cordillera Real in Ecuador represent remnants of such Jurassic segments that experienced collision (fig. 1). The Salado terrane in Ecuador consists of interbedded Upper Jurassic turbiditic metasedimentary rocks and mafic lavas with associated deformed granitoids (Litherland et al. 1994) sandwiched between the Jurassic Abitagua batholith and the Permo-Triassic Loja terrane (Spikings et al. 2015). Detrital zircons from a metasandstone provided zircon ages similar to the mica schists from Colombia, with peak ages in the Mesoproterozoic, Neoproterozoic, and Jurassic (Cochrane et al. 2014*a*). This terrane has been interpreted as having formed in an extensional arc setting limited to the east by the Cosanga fault that separates them from undeformed Jurassic granitoids and the Amazon foreland. During the Late Jurassic to Early Cretaceous this terrane also experienced a relatively higher-pressure collisional event (Massone and Toulkeridis 2010). Such along-strike variation in the tectonic evolution of the margin reflects both the aforementioned Triassic extension and the oblique convergence experienced by the South American continental margin during the Jurassic. In such a scenario, the Otú-Pericos marks the site of oblique subduction and collision of the Tahamí terrane with the Pangea margin. Following such events, the Otú-Pericos fault changed to a strike-slip suture that allowed the final juxtaposition of the Tahamí and Chibcha terrane (Bayona et al. 2006, 2010; Pindell and Kennan 2009). This tectonic evolution suggests that the Chibcha and Tahamí are parautochthonous terranes to the western margin of South America, as previously suggested by Bayona et al. (2010) and Martens et al. 2014).

Conclusions

New U-Pb zircon ages combined with Hf isotopes reveal that the Tierradentro gneisses and amphibolites, previously considered as part of the Grenville event of the Colombian Andes, are actually the record of Permo-Triassic subduction and extension processes that affected western Pangea. The Tierradentro unit is limited by the Otú-Pericos fault that forms the eastern border of a Jurassic sequence that includes mica schists in which their younger detrital zircons were dated at ca. 162 Ma. Such Jurassic rocks, until now undetected in the Central Cordillera of Colombia, can be correlated to the south with the Salado belt in Ecuador. Initial Hf signatures of the Jurassic detrital zircons are distinct from the nearby magmatic rocks of the same age, which suggest sources far from those located at the western margin of Colombia and Ecuador.

ACKNOWLEDGMENTS

This research was supported by Fundação de Amparo à Pesquisa do Estado de São Paulo from Brazil (FAPESP; grants 2010/19068-6 and 2012/14396-0). We acknowledge M. Lara for his support during field work, D. Gómez for his help with mineral identification, G. de Souza Pereira for her comments on this article, and J. C. Piedrahita and J. S. Jaramillo for figure editing. C. Bustamante strongly acknowledges J. D. Vervoort for his support at the Geoanalytical Lab at Washington State University; D. Wilford and C. Fisher for their assistance during isotope geochemistry analyses; and R. Conrey, L. Wagoner, and C. Knaack for their support during the X-ray fluorescence and inductively coupled plasma mass spectrometry analyses. The comments of D. B. Rowley, U. Martens, and an anonymous reviewer helped us to improve the manuscript.

REFERENCES CITED

Bayona, G.; Jiménez, G.; Silva, C.; Cardona, A.; Montes, C.; Roncancio, J.; and Cordani, U. 2010. Paleomagnetic data and K-Ar ages from Mesozoic units of the Santa Marta massif: a preliminary interpretation for block rotation and translations. J. South Am. Earth Sci. 29: 817–831.

Bayona, G.; Rapalini, V.; and Constazo-Alvarez, V. 2006. Paleomagnetism in Mesozoic rocks of the northern Andes and its implications in Mesozoic tectonics of northwestern South America. Earth Planets Space 58: 1255–1272.

Blanco-Quintero, I. F.; García-Casco, A.; Toro, L. M.; Moreno, M.; Ruiz, E. C.; Vinasco, C. J.; Cardona, A.; Lázaro, C.; and Morata, D. 2014. Late Jurassic terrane collision in the northwestern margin of Gondwana (Cajamarca Complex, eastern flank of the Central Cordillera, Colombia). Int. Geol. Rev. 56:1852–1872.

Boekhout, F.; Spikings, R.; Sempere, T.; Chiaradia, M.; Ulianov, A.; and Schaltegger, U. 2012. Mesozoic arc magmatism along the southern Peruvian margin during Gondwana breakup and dispersal. Lithos 146/147: 48–64.

Bustamante, C.; Archanjo, C.; Cardona, A.; Valencia, V.; and Vervoort, J. 2016. Late Jurassic to Early Cretaceous plutonism in the Colombian Andes: a record of long-term arc maturity. Geol. Soc. Am. Bull. 128:1762–1779, doi:10.1130/B31307.1.

Cardona, A.; Valencia, V.; Garzón, A.; Montes, C.; Ojeda, C.; Ruiz, J.; and Weber, M. 2010. Permian to Triassic I to S-type magmatic switch in the northeast Sierra Nevada de Santa Marta and adjacent regions, Colombian Caribbean: tectonic setting and implications with Pangea paleogeography. J. South Am. Earth Sci. 29: 772–783.

Cardona-Molina, A.; Cordani, U. G.; and Macdonald, W. 2006. Tectonic correlations of pre-Mesozoic crust from the northern termination of the Colombian Andes, Caribbean region. J. South Am. Earth Sci. 21:337–354.

Chang, Z.; Vervoort, J. D.; McClelland, W. C.; and Knaack C. 2006. U-Pb dating of zircon by LA-ICP-MS. Geochem. Geophys. Geosyst. 7:1–14.

Cochrane, R.; Spikings, R.; Gerdes, A.; Ulianov, A.; Mora, A.; Villagómez, D.; Putlitz, B.; and Chiaradia, M. 2014*a*. Permo-Triassic anatexis: continental rifting and the disassembly of western Pangaea. Lithos 190/191:383–402.

Cochrane, R.; Spikings, R.; Gerdes, A.; Winkler, W.; Ulianov, A.; Mora, A.; and Chiaradia, M. 2014*b*. Distinguishing between in-situ and accretionary growth of continents along active margins. Lithos 202/203: 382–394, doi:10.1016/j.lithos.2014.05.031.

Coney, P. J.; Jones, D. L.; and Monger, J. W. H. 1980. Cordilleran suspect terranes. Nature 288:329–333.

Cordani, U.; Cardona, A.; Jimenez, D. M.; Liu, D.; and Nutman, A. 2005. Geochronology of Proterozoic basement inliers in the Colombian Andes: tectonic history of remnants of a fragmented Grenville belt. Geol. Soc. Lond. Spec. Publ. 246:329–346.

Cuadros, F. A.; Botelho, N. F.; Ordóñez-Carmona, O.; and Matteini, M. 2014. Mesoproterozoic crust in the San Lucas Range (Colombia): an insight into the crustal evolution of the northern Andes. Precambrian Res. 245: 186–206.

Dickinson, W. R., and Lawton, T. F. 2001. Carboniferous to Cretaceous assembly and fragmentation of México. Geol. Soc. Am. Bull. 113:1142–1160.

DuFrane, S. A.; Vervoort, J. D.; and Hart, G. L.; 2007. Uncertainty of Hf isotope analysis in zircon using LA-MC-ICPMS techniques: full disclosure. Geochim. Cosmochim. Acta 71:A241.

Gaschnig, R. M.; Vervoort, J. D.; Lewis, R.; and McClelland, W. 2010. Migrating magmatism in the northern US Cordillera: in situ U-Pb geochronology of the Idaho batholith. Contrib. Mineral. Petrol. 159:863–883.

Goodge, J. W., and Vervoort, J. D. 2006. Origin of Mesoproterozoic A-type granites in Laurentia: Hf isotope evidence. Earth Planet. Sci. Lett. 243:711–731.

Howell, D. G. 1995. Principles of terrane analysis: new applications for global tectonics. 2nd ed. London, Chapman & Hall.

Ibáñez-Mejía, M.; Ruiz, J.; Valencia, V.; Cardona, A.; Gehrels, G.; and Mora, A. 2011. The Putumayo Orogen of Amazonia and its implications for Rodinia reconstructions: new U-Pb geochronological insights into the Proterozoic tectonic evolution of northwestern South America. Precambrian Res. 191:58–77.

Kerr, A. C.; Marriner, G. F.; Tarney, J.; Nivia, A.; Saunders, A. D.; Thirlwall, M. F.; and Sinton, C. W. 1997. Cretaceous basaltic terranes in Western Colombia: elemental, chronological and Sr-Nd isotopic constraints on petrogenesis. J. Petrol. 38:677–702.

Kroonenberg, S. 1982. A Grenvillian granulite belt in the Colombian Andes and its relations to the Guiana Shield. Geol. Mijnb. 61:325–333.

Leal-Mejía, H. 2011. Phanerozoic gold metallogeny in the Colombian Andes: a tectono-magmatic approach. PhD dissertation, Universitat de Barcelona.

Litherland, M.; Aspden, J. A.; and Jemielita, R. A. 1994. The metamorphic belts of Ecuador. Keyworth, British Geological Survey.

Ludwig, K. R. 2003. Isoplot 3.00. Berkeley, Berkeley Geochronology Center Spec. Publ. 4.

Marquinez, G., and Núñez, A. 1998. Catálogo de las unidades litoestratigráficas de Colombia: Neises y anfibolitas de Tierradentro. Bogotá, Ingeominas.

Martens, U.; Restrepo, J. J.; Ordóñez-Carmona, O.; and Correa-Martinez, A. M. 2014. The Tahamí and Anacona terranes of the Colombian Andes: missing links between the South American and Mexican Gondwana margins. J. Geol. 122:507–530.

Massone, H. J., and Toulkeridis, T. 2010. Widespread relics of high-pressure metamorphism confirm major terrane accretion in Ecuador: a new example from the Northern Andes. Int. Geol. Rev. 54:67–80.

Maya, M., and González, H. 1995. Unidades litodémicas en la Cordillera Central de Colombia. Bol. Geol. 35:43–57.

Noble, S. R.; Aspden, J. A.; and Jemelita, R. 1997. Northern Andean crustal evolution: new U-Pb geochronological constraints from Ecuador. Geol. Soc. Am. Bull. 109: 789–798.

Núñez, A. 2001. Mapa Geológico del Departamento del Tolima escala 1 : 250.000. Memoria explicativa. Bogotá, Ingeominas, 101 p.

Ordóñez-Carmona, O.; Restrepo, J. J.; and Pimentel, M. M. 2006. Geochronological and isotopical review of pre-Devonian crustal basement of the Colombian Andes. J. South Am. Earth Sci. 21:372–382.

Pindell, J. L., and Kennan, L. 2009. Tectonic evolution of the Gulf of Mexico, Caribbean and northern South America in the mantle reference frame: an update. *In* James, K. H.; Lorente, M. A.; and Pindell, J., eds. The origin and evolution of the Caribbean Plate. Geol. Soc. Lond. Spec. Publ. 328:1–56.

Ramos, V. 2009 Anatomy and global context of the Andes: main geologic features and the Andean orogenic cycle. *In* Kay, S. M.; Ramos, V. A.; Dickinson, W. D., eds. Backbone of the Americas: shallow subduction, plateau uplift, and ridge and terrane collision. Geol. Soc. Am. Mem. 204:31–66.

Restrepo, J. J.; Ordóñez-Carmona, O.; Armstrong, R.; and Pimentel, M. M. 2011. Triassic metamorphism in the northern part of the Tahamí Terrane of the central cordillera of Colombia. J. South Am. Earth Sci. 32:497–507.

Restrepo, J. J., and Toussaint, J. F. 1988. Terranes and continental accretion in the Colombian Andes. Episodes 3:189–193.

Restrepo-Pace, P. A.; Ruiz, J.; Gehrels, G.; and Cosca, M. 1997. Geochronology and Nd isotopic data of Grenville-age rocks in the Colombian Andes: new constraints for Late Proterozoic–Early Paleozoic paleocontinental reconstructions of the Americas. Earth Planet. Sci. Lett. 150:427–441.

Riel, N.; Guillot, S.; Jaillard, E.; Martelat, J. E.; Paquette, J. L.; Schwartz, S.; Goncalves, P.; et al. 2013. Metamorphic and geochronogical study of the Triassic El Oro metamorphic complex, Ecuador: implications for high-temperature metamorphism in a forearc zone. Lithos 156–159:41–68.

Rodríguez, G.; Zapata, G.; Arango, M. I.; and Bermúdez, J. G. 2017. Caracterización petrográfica, geoquímica y geocronología de rocas granitoides Pérmicas al occidente de La Plata y Pacarní–Huila, Valle Superior del Magdalena–Colombia. Bol. Geol. 39:41–68.

Rubatto, D. 2002. Zircon trace element geochemistry: partitioning with garnet and the link between U-Pb ages and metamorphism. Chem. Geol. 184:123–138.

Sarmiento-Rojas, L. F.; Van Wess, J. D.; and Cloetingh, S. 2006. Mesozoic transtensional basin history of the Eastern Cordillera, Colombian Andes: inferences from tectonic models. J. South Am. Earth Sci. 21:383–411, doi:10.1016/j.jsames.2006.07.003.

Sláma, J.; Košler, J.; Condon, D. J.; Crowley, J. L.; Gerdes, A.; Hanchar, J. M.; Horstwood, M. S. A.; et al. 2008. Plešovice zircon: a new natural reference material for U-Pb and Hf isotopic microanalysis. Chem. Geol. 249: 1–35.

Spikings, R.; Cochrane, R.; Villagómez, D.; van der Lelij, R.; Vallejo, C.; Winkler, W.; and Beate, B. 2015. The geological history of northwestern South America: from Pangaea to the early collision of the Caribbean Large Igneous Province (290–75 Ma). Gondwana Res. 27:95–139.

Torres, R.; Ruiz, J.; Patchett, P. J.; and Grajales, J. M. 1999. A Permo-Triassic continental arc in eastern Mexico: tectonic implications for reconstructions of southern North America. *In* Bartolini, C.; Wilson, J. L.; and Lawton, T. F., eds. Mesozoic sedimentary and tectonic history of north-central Mexico. Geol. Soc. Am. Spec. Pap. 340:191–196.

Toussaint, J. F. 1995. Evolución Geológica de Colombia: Triásico–Jurásico. Medellín, Editorial Universidad Nacional, 277 p.

Toussaint, J. F., and Restrepo, J. J. 1989. Acreciones sucesivas en Colombia: un nuevo modelo de evolución geológica. Memorias V Congreso Colombiano de Geología, p. 127–146.

van der Lelij, R.; Spikings, R.; Ulianov, A.; Chiaradia, M.; and Mora, A. 2016. Palaeozoic to Early Jurassic history of the northwestern corner of Gondwana, and implications for the evolution of the Iapetus, Rheic and Pacific Oceans. Gondwana Res. 31:271–294, doi:10.1016/j.gr.2015.01.011.

Vanegas, J.; Cardona, J.; Blanco-Quintero, I.; and Valencia, V. 2014. Late Jurassic crustal thickening in the Mesozoic arc of Ecuador and Colombia: implications on the evolution of continental arcs. Am. Geophys. Union Fall Meeting 2015, abstract T11C-4584.

Vervoort, J. D.; Kemp, A. I. S.; Fisher, C.; and Bauer, A. 2015. The rock record has it about right—no significant continental crust formation prior to 3.8 Ga. Am. Geophys. Union Fall Meeting 2015, abstract V43D-05.

Vervoort, J. D., and Patchett, P. J. 1996. Behavior of hafnium and neodymium isotopes in the crust: constraints from Precambrian crustally derived granites. Geochim. Cosmochim. Acta 60:3717–3733.

Vervoort, J. D.; Patchett, P. J.; Soderlund, U.; and Baker, M. 2004. Isotopic composition of Yb and the determination of Lu concentrations and Lu/Hf ratios by isotope dilution using MC-ICPMS. Geochem. Geophys. Geosyst. 5:15.

Vesga, C. J., and Barrero, D. 1978. Edades K/Ar en rocas ígneas y metamórficas de la Cordillera Central de Colombia y su implicación geológica. Bogota, II Congreso Colombiano de Geología: Resúmenes.

Villagómez, D.; Spikings, R.; Magna, T.; Kammer, A.; Winkler, W.; and Beltrán, A. 2011. Geochronology: geochemistry and tectonic evolution of Western and Central Cordilleras of Colombia. Lithos 125:875–896.

Vinasco, C.; Cordani, U.; González, H.; Weber, M.; and Peláez, C. 2006. Geochronological, isotopic, and geochemical data from Permo-Triassic granitic gneisses and granitoids of the Colombian Central Andes. J. South Am. Earth Sci. 21:355–371.

Zapata-García, G.; Rodríguez-García, G.; and Arango-Mejía, M. I. 2017. Petrografía, geoquímica y geocronología de rocas metamórficas aflorantes en San Francisco Putumayo y la vía Palermo-San Luis asociadas a los complejos La Cocha–Río Téllez y Aleluya. Bol. Cienc. Tierra 41:47–64.